

## Electronic structures of NiO, CoO, and FeO studied by 2*p* core-level x-ray photoelectron spectroscopy

Geunseop Lee and S.-J. Oh\*

*Department of Physics, Seoul National University, Seoul 151-742, Korea*

(Received 25 June 1990; revised manuscript received 12 March 1991)

We have analyzed the satellite structures of the transition-metal 2*p*<sub>3/2</sub> core-level photoemission spectra of NiO, CoO, and FeO within the charge-transfer cluster model. The spectra can be fitted with reasonable values of the parameters of the model, which show the expected trend along the transition-metal series as well as along the ligand series including halogen and oxygen. The values of the *d-d* electron correlation energy *U* and the charge-transfer energy  $\Delta$  from the ligand to the metal 3*d* level in the valence electronic structures are then estimated from these parameter values. We confirm that the large-*U* value is important for the insulating properties of these monoxides, but the band gap is not determined by *U*, but rather by  $\Delta$ . This supports the recent proposal that these oxides are not Mott-Hubbard insulators in the original sense, but belong to the charge-transfer-type insulators. We also calculate the magnitudes of the band gaps with our parameter values, and they are in fair agreement with experimental values and show the correct trend.

### I. INTRODUCTION

The 3*d* transition-metal compounds have been the subject of study<sup>1-6</sup> for many years because of their diverse physical properties. In spite of their apparently similar electronic structures having unfilled 3*d* shells, their electrical conductivities vary widely from metallic to insulating behaviors, and they also show diverse magnetic properties. According to the elementary independent electron band theory, most of the 3*d* transition-metal compounds should be metallic because of their unfilled 3*d* shells. Some of them (CuS, NiSe, NiTe, CoS, etc.) are indeed metals, but there are many compounds which are insulators (NiF<sub>2</sub>, NiO, CuO, etc.), or subject to the metal-to-nonmetal transition (NiS, V<sub>2</sub>O<sub>3</sub>, etc.) depending on the temperature or the pressure.

To solve this apparent contradiction, Mott<sup>1</sup> and Hubbard<sup>2</sup> considered the following charge fluctuation of the interatomic type:

$$d_A^n d_B^n \rightarrow d_A^{n-1} d_B^{n+1}, \quad (1)$$

where *A* and *B* label the transition-metal sites. They proposed that for electron conduction to occur, the energy required for the above process should be less than the 3*d* band width. That is, for some transition-metal compounds the large value of the *d-d* Coulomb and exchange interaction energy *U* (*U* > *w*, where *w* is the 3*d* dispersive band width) makes it impossible for the above charge fluctuation to occur so that the compounds become insulators in spite of their unfilled *d* shells (Mott-Hubbard insulators). When *U* is smaller than *w*, the compounds will be metals as predicted in the elementary band theory.

The Mott-Hubbard theory can explain the properties of many insulating compounds of the early 3*d* transition metals such as Ti and V, but for the late 3*d* transition-metal compounds it is not quite satisfactory. First of all,

the theory requires a wide range of change for the value of *U* depending on the anions, from the higher value of about 8–10 eV in insulating compounds such as NiO (Refs. 7 and 8) to the lower value of at most the same order of magnitude as the 3*d* band dispersive width *w* (which is usually believed<sup>3</sup> to be less than 1 eV) in metallic compounds such as NiS. Also the conductivity gap seems to be related directly to the electronegativity of the anion in these late 3*d* transition-metal compounds.<sup>9</sup> Such a big change of *U* values and the strong dependence of the band gap upon the anions with the same metal cations are rather unlikely, since the 3*d* electrons of the metal ions are fairly localized and therefore the *d-d* Coulomb correlations and the *d-d* gaps are not believed to be dependent so much upon the anions.

Recently a theory has been proposed<sup>10</sup> that can describe the band gaps and the electronic structures of transition-metal compounds consistently by modifying the conventional Mott-Hubbard model. This theory considers explicitly two types of charge fluctuation for a possible conduction mechanism. One is the interatomic polar fluctuation or the conventional Mott-Hubbard-type fluctuation, as described by Eq. (1). The other type of fluctuation which has been introduced in this theory is the charge-transfer process between the ligand state and the metal *d* level

$$d^n \rightarrow d^{n+1} \underline{L}, \quad (2)$$

where  $\underline{L}$  denotes a hole in the anion valence band. This type of process requires the charge-transfer energy  $\Delta$ , which has been assumed to be so large compared with the *d-d* Coulomb correlation energy *U* that this process has been neglected by Mott, Hubbard, and other researchers. The conductivity gap is determined by the minimum energy for the creation of one electron and one hole which are uncorrelated from the ground state. The theory uses the Anderson impurity Hamiltonian containing the pa-

parameter  $T$  for the hybridization strength between the ligand band and the metal  $3d$  electron, and the anion valence bandwidth  $W \approx 4$  eV, as well as the  $d-d$  Coulomb energy  $U$ ,  $d$ -band dispersional width  $w$ , and the charge-transfer energy  $\Delta$ . According to this theory, the transition-metal compounds can be classified as metals ( $U < w$  or  $\Delta < W/2$ ), insulators in the conventional Mott-Hubbard regime ( $w < U < \Delta$ ), and insulators in the charge-transfer regime ( $W/2 < \Delta < U$ ).

Recent progress in the electron spectroscopic technique and its interpretation allows direct determinations of essentially all these parameter values from the experimental data. The valence-band spectrum of x-ray photoelectron spectroscopy (XPS) or ultraviolet photoelectron spectroscopy (UPS) measures the energies of various ionized states, and bremsstrahlung isochromat spectroscopy (BIS) can measure the electron affinity states. By a proper analysis of these spectra, one can determine the values of  $\Delta$ ,  $U$ ,  $W$ , and  $w$  as shown in Fig. 1. Results on NiO (Refs. 8, 7, and 11) and NiS (Ref. 12) show that the Ni  $d-d$  Coulomb energy  $U$  does not change very much from compound to compound, and remains much larger than the  $d$ -band dispersional width  $w$  even for metallic NiS, supporting the predictions of this theory.

Core-level XPS can be used also to determine similar parameter values. Many  $3d$  transition-metal compounds show complicated satellite structures in the  $2p$  core-level XPS spectra. In the case of insulating copper dihalides, these satellite structures have been successfully explained<sup>13</sup> by a model that is based on the same physical picture and uses parameters such as  $\Delta$ ,  $T$ , and  $U$  as in the theory of the valence UPS and BIS spectra analyses mentioned above. There is in this model an additional parameter  $Q$ , the Coulomb attraction energy between a core hole and the  $3d$  electron, since it describes the core-level

photoelectron spectra. By fitting the positions and the intensities of the main peak and the satellites in the  $2p$  core-level spectra, one can get the values of the parameters  $\Delta$ ,  $T$ ,  $U$ , and  $Q$ , which in turn give information on the valence electronic structures of the compounds. Later this model, which we will call the "charge-transfer model," has been applied successfully to account for the  $2p$  core-level photoemission spectra of other heavy transition-metal (Ni, Co, Fe, and Mn) dihalides,<sup>14,15</sup> and the obtained parameter values show the expected trends not only along the ligand series but also along the transition-metal series. This method of using core-level XPS to study valence-band parameters has the advantage of being simple and easy to interpret compared with the combined analyses of valence-band XPS and BIS. However, as we will show later in this paper, since the parameters  $\Delta$ ,  $U$ , and  $T$  are *effective* parameters of model Hamiltonians, their values obtained from the analysis of the core-level XPS may not be the same as those describing the valence-band electronic structures, although their physical meanings are similar. We will discuss their relations in detail, and show how to obtain the parameter values describing the valence-band electronic structures from the core-level parameter values.

In this paper, we report the results of our study on the  $2p$  core-level XPS spectra of the late transition-metal monoxides NiO, CoO, and FeO. These monoxides are interesting especially because they all have been known as typical Mott-Hubbard insulators. By analyzing the satellite structures of the measured  $2p$  core-level spectra in terms of the charge-transfer model, we obtain the values of the parameters such as the effective Coulomb correlation energy and the charge-transfer energy for these compounds. These parameter values are found to differ somewhat from those obtained by the analysis of the valence-band spectra. We derive the relation between these two sets of parameters, and based on these values we discuss the valence-band electronic structures of these oxides including the nature of the band gap.

The organization of this paper is as follows. In Sec. II we describe the samples used and the experimental procedures to obtain the XPS spectra. In Sec. III, the model calculations to interpret the  $2p$  core-level spectra are described and the parameter values of the model are determined from the fit of the experimental  $2p$  XPS data. In Sec. IV we try to derive information on the valence electronic structures from the core-level parameters obtained in Sec. III. We finally summarize the conclusions of this paper in Sec. V.

## II. MATERIALS AND EXPERIMENTAL PROCEDURES

The materials we studied are late transition-metal monoxides NiO, CoO, and FeO. They all have the NaCl structure, and each transition-metal cation is surrounded by the octahedron of six nearest-neighbor oxygen ions. In the octahedral symmetry ( $O_h$ ), the metal  $3d$  level is split into  $e_g$  (doublet) and  $t_{2g}$  (triplet) levels with the energy separation  $10Dq$  by the crystal field from the surrounding anions.<sup>16</sup> These monoxides have a ground state of the high spin configuration since the exchange energy

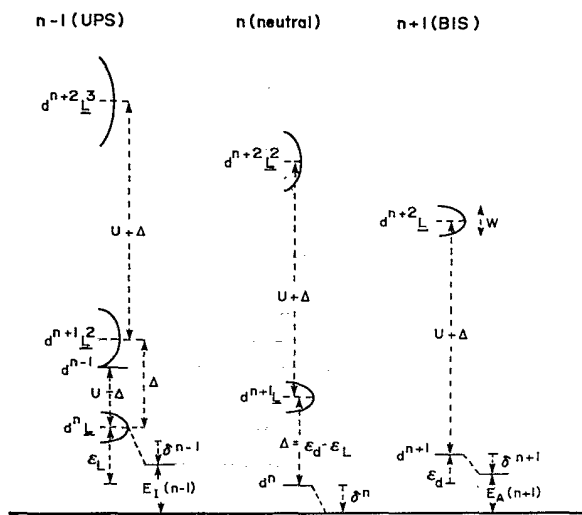


FIG. 1. Total energy diagram indicating the states and energies involved in describing the valence electron structures of the transition-metal compounds proposed by Zaanen, Sawatzky, and Allen (taken from Ref. 10).

is larger than the crystal-field-splitting energy  $10Dq$ . Thus the ground-state configuration for each metal ion is<sup>17,18</sup>  ${}^3A_{2g}(t_{2g}^6e_g^2)$  for  $\text{Ni}^{2+}$  ( $d^8$ ),  ${}^4T_{1g}(t_{2g}^5e_g^2)$  for  $\text{Co}^{2+}$  ( $d^7$ ), and  ${}^5T_{2g}(t_{2g}^4e_g^2)$  for  $\text{Fe}^{2+}$  ( $d^6$ ) ions, respectively. Of the materials we studied, CoO was prepared in the form of a disk pellet by pressing commercially obtained powders (Johnson Matthey Co., purity >99.9%), and NiO and FeO were single crystals. The experiments were performed with the XPS spectrometer manufactured by VSW Scientific Instruments Ltd., which was equipped with a 150-mm mean radius concentric hemispherical analyzer (CHA) with multichannel detection system and Mg/Al twin-anode x-ray sources. Mg  $K\alpha$  x ray ( $h\nu=1253.6$  eV) was used for the spectra of NiO and CoO, whereas Al  $K\alpha$  x ray ( $h\nu=1486.6$  eV) was used for the  $2p$  core-level spectra of CoO to avoid overlapping Auger peaks. The base pressure of the photoelectron spectroscopy chamber was better than  $7\times 10^{-10}$  Torr, and the crystalline samples were cut *in situ* to get fresh surfaces. The overall resolution of the experiment was  $\sim 1.3$  eV.

### III. MODEL CALCULATIONS AND EXPERIMENTAL RESULTS

We have performed the charge-transfer model calculations for  $d^6$ ,  $d^7$ , and  $d^8$  configurations in the cluster approximation. The full impurity calculation, which takes into account the ligand band dispersion, is prohibitively expensive and almost impossible to do for the case of more than two  $d$  holes in the ground state. Fortunately, when  $\Delta$  and  $U$  are large compared with the bandwidth ( $U > \Delta > W/2 \approx 2$  eV), it was shown that the cluster approach neglecting the ligand level energy dispersion is a good approximation to the full impurity calculation.<sup>14</sup> The model Hamiltonians we are going to use for NiO, CoO, and FeO are similar to those used earlier for the transition-metal dihalides in Ref. 15, but we now extend them to include the effects of the crystal-field splittings. For Co and Fe compounds, the  $t_{2g}$  holes are involved for the model as well as the  $e_g$  holes. In the previous model for dihalides,<sup>15</sup> we have neglected the difference between these two orbitals and assumed that they are degenerate in energy and the transfer integrals  $T$ 's are the same. However, the  $t_{2g}$  orbitals are  $\pi$  bonding and  $e_g$  orbitals are  $\sigma$  bonding, so we expect the hybridization strengths of these two orbitals to be different. In fact, the band-structure calculation<sup>3</sup> shows that  $T(t_{2g})$  is about half of  $T(e_g)$ . So we set in our current calculation

$$\begin{aligned} T(e_g) &\equiv \langle e_g | H | L_{e_g} \rangle = T, \\ T(t_{2g}) &\equiv \langle t_{2g} | H | L_{t_{2g}} \rangle = 0.5T. \end{aligned} \quad (3)$$

The energy difference  $10Dq$  between  $e_g$  and  $t_{2g}$  levels is about 1 eV for the divalent transition-metal compounds, but most of this energy difference comes from the covalency effect.<sup>19</sup> The value of  $10Dq$  we should use in this model is the noncovalent contribution, which is usually quite small.<sup>20</sup> So we set  $10Dq(\text{noncovalent})=0$  (i.e.,  $e_g$  and  $t_{2g}$  orbitals are assumed to be degenerate without hy-

bridization) in our model for simplicity. The other parameters used here are the charge-transfer energy  $\Delta_1$ , the  $3d$ - $3d$  Coulomb interaction energy  $U_1$ , and the metal  $2p$  hole- $3d$  electron attraction energy  $Q$ . Note that we have used the notations  $\Delta_1$  and  $U_1$  to distinguish them from the parameters  $\Delta$  and  $U$  obtained from the valence-band UPS and BIS analyses mentioned in Sec. I. In previous work<sup>14,15</sup> these parameters from the core-level analysis were also called  $\Delta$  and  $U$  without distinguishing them from the valence-band parameters. However, as mentioned briefly in Sec. I, they are determined by different physical processes so that their values may well be different, although the physical concepts are similar (see Sec. IV for detailed discussions). The model Hamiltonians thus determined for NiO, CoO, and FeO are described in Table I.

The initial ground state  $|\Psi_G\rangle$  and the eigenstates of the final state  $|\Psi_f\rangle$  are obtained by diagonalizing the model Hamiltonians in the initial and final states, respectively. Since the photoemission process in XPS can be taken as a sudden process, we can calculate the intensities of the photoemission peaks using the sudden approximation. The peak intensity of each final state is obtained by the square of the overlap integral between  $|\Psi_f\rangle$  and  $|\underline{c}\Psi_G\rangle$ , where  $|\underline{c}\Psi_G\rangle$  denotes the state with an electron removed from the core-level  $c$  ( $2p$  hole in this case) while leaving other orbitals frozen. We now change the values of parameters  $\Delta_1$ ,  $U_1$ ,  $Q$ , and  $T$  to make the theoretical peak separations and intensity ratios as close to the experimental  $2p$  core-level spectra as possible. To reduce the number of free parameters, we imposed the atomic relation<sup>21</sup>  $\Delta_1=0.7Q$  in the theoretical calculations. We have fitted only the  $2p_{3/2}$  part of our experimental spectra, because the  $2p_{1/2}$  spectra are sometimes affected by the strong interference effect between the threshold Coster-Kronig decay and the valence electron rearrangement after the  $2p$  core hole creation.<sup>22</sup> Even in the  $2p_{3/2}$  spectra, the peaks assigned as the main or satellite peaks cannot be fitted with single peaks, presumably because of their complicated multiplet structures. Since we do not know the exact positions and intensities of multiplets for each final state and the multiplet effect is not included in our model, we mimicked them by superposing several Lorentzian peaks for each final state.

In Figs. 2, 3, and 4, we show the experimental  $2p_{3/2}$  spectra of NiO, CoO, and FeO along with the best theoretical fit for each spectrum. The experimental spectra were found to be broadened somewhat by the charging effect, since no neutralizing gun was used for these very good insulating samples. However, this poses no essential problem for our purpose, because we are only interested in the energy separation and the intensity ratio between the main peak and satellites. In the experimental spectra, the inelastic background was subtracted from the raw data in the common way, in which the ratio of the ejected electrons with energy loss to those without energy loss is assumed to be constant and independent of the amount of the energy loss.<sup>23</sup> The theoretical curve is convoluted with the Gaussian broadening for the instrumental resolution and the effect of charging, and with the Lorentzian broadening to mimic the lifetime and the mul-

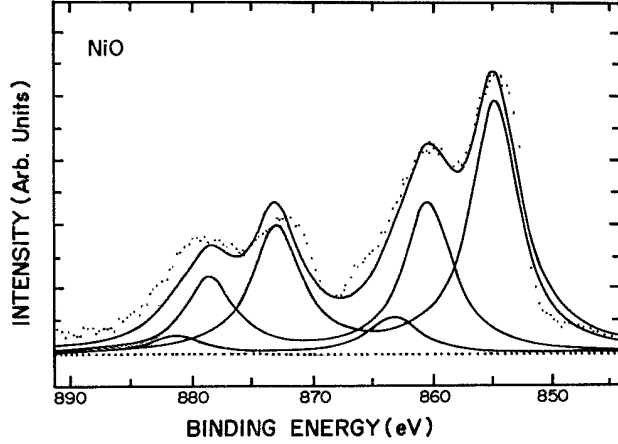


FIG. 2. The experimental Ni  $2p$  core-level XPS spectra (dots) of NiO and the theoretical fit (solid line) of the  $2p_{3/2}$  level.

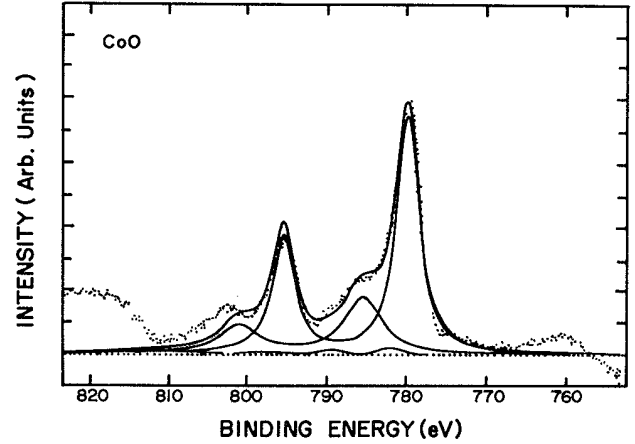


FIG. 3. The experimental Co  $2p$  core-level XPS spectra (dots) of CoO and the theoretical fit (solid line) of the  $2p_{3/2}$  level.

triplet effects. In Table II we list the optimally chosen parameter values  $\Delta_1$ ,  $U_1$ ,  $Q$ , and  $T$  for each transition-metal monoxide. For comparison, we also list the parameter values for the transition-metal dihalides, which are redetermined within our revised model using the experimental spectra in Ref. 15. We tried to use the same

values of  $T$  and  $U_1$  for the same metal cation independent of the anions as before.<sup>15</sup> (exception: the  $U_1$  value for NiO is chosen to be a little different from those for Ni dihalides to obtain a slightly better fit.) The parameter values for Co and Fe dihalides are somewhat different from those of Ref. 15, because of our inclusion of the

TABLE I. Basis states and Hamiltonian matrix elements in the initial state within the charge-transfer cluster model. The matrices are all symmetric and their elements are given only for the right upper part. The numbers (1), (2) represent  $x^2-y^2$  and  $3z^2-r^2$  for  $e_g$  orbitals or two of  $xy, yz, zx$  for  $t_{2g}$  orbitals. The model Hamiltonian for the final state (after  $2p$  photoemission) is obtained by replacing  $\Delta_1$  with  $\Delta_1 - Q$  in the diagonal matrix elements. All off-diagonal elements are assumed unchanged by the hole created. (Here  $e_g$  and  $t_{2g}$  represent  $d$  holes.)

NiO	$ 1\rangle =  e_g^2\rangle$ , $ 2\rangle = \frac{1}{\sqrt{2}}[ e_g(1)\underline{L}_{e_g(2)}\rangle +  e_g(2)\underline{L}_{e_g(1)}\rangle]$ , $ 3\rangle =  \underline{L}_{e_g(1)}\underline{L}_{e_g(2)}\rangle$ $H_{11} = 0$ , $H_{22} = \Delta_1$ , $H_{33} = 2\Delta_1 + U_1$ $H_{12} = H_{23} = \sqrt{2}T$
CoO	$ 1\rangle =  e_g^2 t_{2g}\rangle$ , $ 2\rangle = \frac{1}{\sqrt{2}}[ e_g(1)t_{2g}\underline{L}_{e_g(2)}\rangle +  e_g(2)t_{2g}\underline{L}_{e_g(1)}\rangle]$ $ 3\rangle =  e_g^2 \underline{L}_{t_{2g}}\rangle$ , $ 4\rangle =  t_{2g}\underline{L}_{e_g(1)}\underline{L}_{e_g(2)}\rangle$ $ 5\rangle = \frac{1}{\sqrt{2}}[ e_g(1)\underline{L}_{e_g(2)}\underline{L}_{t_{2g}}\rangle +  e_g(2)\underline{L}_{e_g(1)}\underline{L}_{t_{2g}}\rangle]$ , $ 6\rangle =  \underline{L}_{e_g(1)}\underline{L}_{e_g(2)}\underline{L}_{t_{2g}}\rangle$ $H_{11} = 0$ , $H_{22} = H_{33} = \Delta_1$ , $H_{44} = H_{55} = 2\Delta_1 + U_1$ , $H_{66} = 3\Delta_1 + 3U_1$ $H_{12} = H_{24} = H_{35} = H_{56} = \sqrt{2}T$ , $H_{13} = H_{25} = H_{46} = T(t_{2g}) = 0.5T$
FeO	$ 1\rangle =  e_g^2 t_{2g}^2\rangle$ , $ 2\rangle = \frac{1}{\sqrt{2}}[ e_g(1)t_{2g}^2 \underline{L}_{e_g(2)}\rangle +  e_g(2)t_{2g}^2 \underline{L}_{e_g(1)}\rangle]$ $ 3\rangle = \frac{1}{\sqrt{2}}[ e_g^2 t_{2g}(1)\underline{L}_{t_{2g}(2)}\rangle +  e_g^2 t_{2g}(2)\underline{L}_{t_{2g}(1)}\rangle]$ , $ 4\rangle =  t_{2g}^2 \underline{L}_{e_g(1)}\underline{L}_{e_g(2)}\rangle$ $ 5\rangle = \frac{1}{2}[(e_g(1)t_{2g}(1)\underline{L}_{e_g(2)}\underline{L}_{t_{2g}(2)}) +  e_g(2)t_{2g}(1)\underline{L}_{e_g(1)}\underline{L}_{t_{2g}(2)}\rangle$ $+  e_g(1)t_{2g}(2)\underline{L}_{e_g(2)}\underline{L}_{t_{2g}(1)}\rangle +  e_g(2)t_{2g}(2)\underline{L}_{e_g(1)}\underline{L}_{t_{2g}(1)}\rangle]$ $ 6\rangle =  e_g^2 \underline{L}_{t_{2g}(1)}\underline{L}_{t_{2g}(2)}\rangle$ , $ 7\rangle = \frac{1}{\sqrt{2}}[ t_{2g}(1)\underline{L}_{e_g(1)}\underline{L}_{e_g(2)}\underline{L}_{t_{2g}(2)}\rangle +  t_{2g}(2)\underline{L}_{e_g(1)}\underline{L}_{e_g(2)}\underline{L}_{t_{2g}(1)}\rangle]$ $ 8\rangle = \frac{1}{\sqrt{2}}[ e_g(1)\underline{L}_{e_g(2)}\underline{L}_{t_{2g}(1)}\underline{L}_{t_{2g}(2)}\rangle +  e_g(2)\underline{L}_{e_g(1)}\underline{L}_{t_{2g}(1)}\underline{L}_{t_{2g}(2)}\rangle]$ $ 9\rangle =  \underline{L}_{e_g(1)}\underline{L}_{e_g(2)}\underline{L}_{t_{2g}(1)}\underline{L}_{t_{2g}(2)}\rangle$ $H_{77} = H_{88} = 3\Delta_1 + 3U_1$ , $H_{99} = 4\Delta_1 + 6U_1$ $H_{12} = H_{24} = H_{35} = H_{57} = H_{68} = H_{89} = \sqrt{2}T$ $H_{13} = H_{25} = H_{36} = H_{47} = H_{58} = H_{79} = \sqrt{2}T(t_{2g}) = \sqrt{2}(0.5T)$

TABLE II. Parameter values and the ground-state  $3d$  occupation number  $\langle n_d \rangle$  determined from the fit of the metal  $2p_{3/2}$  core-level XPS spectra of transition-metal monoxides and dihalides within the charge-transfer model. All energies are in eV.

TM	Compounds	$\Delta_1$	$T$	$U_1$	$Q$	$\langle n_d \rangle$
Ni	NiF <sub>2</sub>	6.5	2.0	5.0	7.0	8.14
	NiO	5.0	2.0	5.3	7.6	8.20
	NiCl <sub>2</sub>	3.6	2.0	5.0	7.0	8.29
	NiBr <sub>2</sub>	2.6	2.0	5.0	7.0	8.39
Co	CoF <sub>2</sub>	8.3	2.1	4.5	6.4	7.11
	CoO	5.7	2.1	4.5	6.4	7.19
	CoCl <sub>2</sub>	4.2	2.1	4.5	6.4	7.28
	CoBr <sub>2</sub>	3.4	1.7	4.5	6.5	7.34
Fe	FeF <sub>2</sub>	9.2	1.9	4.1	5.9	6.16
	FeO	5.6	1.9	4.1	5.9	6.20
	FeCl <sub>2</sub>	4.5	1.9	4.1	5.9	6.26
	FeBr <sub>2</sub>	3.2	1.9	4.1	5.9	6.37

crystal-field effects.  $T$  values become larger, which is reasonable since the  $T$  value in Ref. 15 is sort of the average of  $T(e_g)$  and  $T(t_{2g})$ , and  $\Delta_1$  values are smaller.

The parameter values in Table II show reasonable trends. First, the  $\Delta_1$  values for compounds with the same metal ion show the order of the electronegativity of the ligand, including the oxygen. Second, the  $\Delta_1$  values along the metal ions with the same ligand show the order of the electronegativity of the metal ion. Third, the Coulomb interaction parameters  $U_1$  and  $Q$  increase as we go from Fe to Ni, as expected from the more localized  $3d$  wave functions of the heavier transition-metal ions. And last we note that the magnitude of the hybridization parameter  $T$  is similar to what is needed to give the covalent crystal-field-splitting energy  $10Dq \approx 1$  eV for these compounds.

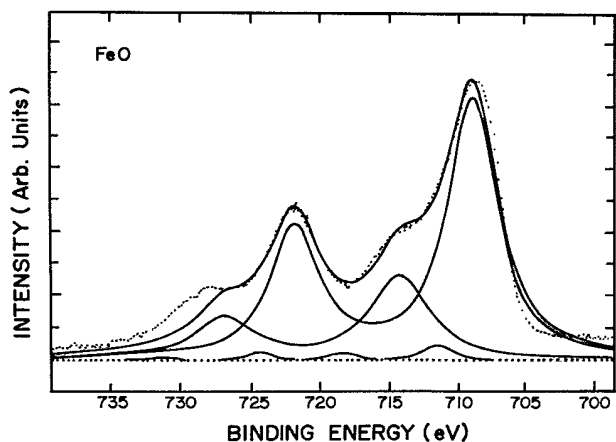


FIG. 4. The experimental Fe  $2p$  core-level XPS spectra (dots) of FeO and the theoretical fit (solid line) of the  $2p_{3/2}$  level.

#### IV. INFORMATION ON THE VALENCE ELECTRONIC STRUCTURES FROM $2p$ XPS ANALYSIS

##### A. $\Delta_1, U_1$ and $\Delta, U$

In previous sections we have described two sets of parameters ( $\Delta, U$  and  $\Delta_1, U_1$ ) which are similar in their physical origins but have subtle differences.  $\Delta$  and  $U$  are parameters describing the valence electronic structure or parameters for the valence-band UPS and BIS analyses, whereas  $\Delta_1$  and  $U_1$  are parameters describing the core- ( $2p$ ) level XPS spectra. Since these are *effective* parameters of the model Hamiltonians and they describe different physical processes, their values may be different.<sup>14,24</sup> In this section, we discuss this issue and the possibility of obtaining information on the valence electronic structures from the analysis of the core-level spectra.

$\Delta$  and  $\Delta_1$  are both parameters representing the energy associated with the charge-transfer process  $d^n \rightarrow d^{n+1}\underline{L}$ , so they both contain the Madelung potentials and the polarization correction. But there are the following two important differences. (i) While  $\Delta$  corresponds to the charge-transferred state, which has no correlation between the ligand hole and the  $d$  electron,  $\Delta_1$  includes the ligand hole and  $d$ -electron correlation effect because it is defined as the energy for the excitonic state in which the transferred  $d$  electron comes from the nearest-neighbor anion and hence the ligand hole and the  $d$  electron can interact. (ii) While  $\Delta$  is defined as the difference in energy between the lowest multiplets of  $d^n$  and  $d^{n+1}\underline{L}$  states,  $\Delta_1$  is more akin to the difference between the lowest multiplet energy of  $d^n$  and the average configuration energy of  $d^{n+1}\underline{L}$  multiplets. Therefore, under the assumption that polarization corrections do not change, we can write

$$\Delta = \Delta_1 + u - E_{\text{Hund}}(d^{n+1}), \quad (4)$$

where  $u$  is the ligand hole- $3d$  electron attraction energy, and  $E_{\text{Hund}}(d^{n+1})$  is the Hund's rule energy for the  $d^{n+1}$  lowest multiplet configuration.

In similar way, we can obtain the relation between the core XPS parameter  $U_1$  and the valence-band  $3d$  electron correlation energy  $U$ , a quantity which is essential for Mott-Hubbard and its generalized theories. They are both effective parameters representing the metal  $d-d$  Coulomb interactions, and contain the polarization energy correction ( $-2E_p$ ) from the bare value of the free ion. But as in the case of the  $\Delta_1$  and  $\Delta$  discussed above, there are some differences. (i) The core-level parameter  $U_1$  includes the hole-electron attraction energy  $u$  whereas the valence-band parameter  $U$  does not, because the latter is defined in the charge fluctuation process that gives rise to the electric conduction. (ii)  $U$  is the energy needed for the charge fluctuation  $2d^n \rightarrow d^{n-1} + d^{n+1}$  so we can write for  $U$

$$U = E(d^{n+1}) + E(d^{n-1}) - 2E(d^n) = U(d^{n-1} \rightarrow d^{n+1}) \quad (5)$$

whereas  $U_1$  in the core-level charge-transfer model is defined as

$$\begin{aligned} U_1 &= [E(d^{n+2}) - E(d^{n+1})] - [E(d^{n+1}) - E(d^n)] \\ &= E(d^{n+2}) + E(d^n) - 2E(d^{n+1}) = U(d^n \rightarrow d^{n+2}), \end{aligned} \quad (6)$$

where we have neglected the excitonic energy  $-2u$  for the moment. That is,  $U$  and  $U_1$  involve a different number of  $d$  electrons, and in free ions the Coulomb interaction energy  $U_0(d^{n-1} \rightarrow d^{n+1})$  is usually larger than  $U_0(d^n \rightarrow d^{n+2})$  for late transition metals. (iii)  $E(d^{n+1})$  and  $E(d^{n-1})$  in Eq. (5) refer to the lowest multiplet energies of the  $d^{n+1}$  and  $d^{n-1}$  configurations, whereas  $E(d^{n+2})$  and  $E(d^{n+1})$  in Eq. (6) refer to the average configuration energies. Therefore, we have to take into account the difference in Hund's rule energies. Taking all these into consideration we can write, assuming the polarization corrections in the solid are the same,

$$U = U_1 + 2u + \Delta U_0 + \Delta E_{\text{Hund}}, \quad (7)$$

where

$$\Delta U_0 = U_0(d^{n-1} \rightarrow d^{n+1}) - U_0(d^n \rightarrow d^{n+2})$$

is the difference of the Coulomb energies in the lowest multiplets of free ions, and

$$\Delta E_{\text{Hund}} = 2E_{\text{Hund}}(d^{n+1}) - E_{\text{Hund}}(d^{n+2})$$

arises from the difference of the Hund's rule energies, and  $u$  is the ligand hole- $3d$  electron attraction energy defined earlier.

The parameters  $u$ ,  $E_{\text{Hund}}$ , and  $\Delta U_0$  in Eqs. (4) and (7) all can be estimated reasonably well. First of all, the ligand hole- $3d$  electron attraction energy  $u$  can be calculated in the same way as in Ref. 14. Here we assume the localized  $3d$  electron and the ligand hole that is localized fully on the nearest-neighboring ring of oxygen ions. We then calculate  $u$  in the point-charge approximation, which treats two point charges in a dielectric medium. In this case, the screening (polarization) can be treated reasonably well in terms of the optical dielectric constant  $\epsilon_\infty$ . The results of our calculation, as well as necessary parameters, are listed in Table III. In this calculation, we used the experimental values<sup>25</sup> of  $\epsilon_\infty$  for NiO and CoO, and the value for FeO was derived from the Clausius-Mossotti relation using the polarizabilities of cation [ $\alpha(\text{Fe}) = 1.13 \text{ \AA}^{-3}$ ] and anion [ $\alpha(\text{O}^{2-}) = 1.84 \text{ \AA}^{-3}$ ]. The Hund's rule energy  $E_{\text{Hund}}$  for each configuration can be calculated from the standard multiplet theory and the tabulated values of the atomic Slater integrals<sup>26</sup>  $F^2(dd)$  and  $F^4(dd)$ . The results of these calculations are listed in Tables III and IV.

The free-atom Coulomb energy values  $U_0$  can be obtained from the ionization potentials tabulated in Moore's table,<sup>27</sup>

$$\begin{aligned} U_0(d^{n-1} \rightarrow d^{n+1}) &= I_M(d^n \rightarrow d^{n-1}) - I_M(d^{n+1} \rightarrow d^n), \\ U_0(d^n \rightarrow d^{n+2}) &= I_M(d^{n+1} \rightarrow d^n) - I_M(d^{n+2} \rightarrow d^{n+1}), \end{aligned} \quad (8)$$

where the  $I_M$ 's are the ionization potentials. Here, however, there is some ambiguity as to what configurations to take for the calculation of  $U_0(d^n \rightarrow d^{n+2})$ . The reason is that  $U_1$  appears in both the initial and the final-state Hamiltonians, and there is an extra core hole in the final state. For example, in the case of NiO, the  $U_1$  in the initial state is certainly related to the ionization potentials of the  $d^{10}$  and  $d^9$  configurations of the Ni atom or ion, whereas in the final state with a  $2p$  core hole, it may be more appropriate to use the ionization potentials of Cu ions in the spirit of the  $Z+1$  approximation. In Table IV we list values of  $\Delta U_0$  calculated in both ways— $\Delta U_0^Z$

TABLE III. Estimate of the charge-transfer energy  $\Delta$  for the valence electronic structure from the core-level parameter  $\Delta_1$  along with the necessary parameters. Here  $R$  is the distance between the transition-metal ion and the oxygen, and other parameters are explained in the text. All energies are in eV.

	$\Delta_1$	$R$ (Å)	$\epsilon_\infty$	$u$	$E_{\text{Hund}}(d^{n+1})$	$\Delta$
NiO	5.0	2.10	5.7	1.2	0.0	6.2
CoO	5.7	2.13	5.3	1.3	1.0	6.0
FeO	5.6	2.16	5.9	1.1	1.8	4.9

TABLE IV. Estimate of the  $d$ - $d$  Coulomb correlation energy  $U$  for the valence electronic structure from the core-level parameter  $U_1$  along with the necessary parameters. The meaning of the parameters is explained in the text, and  $\Delta U_0^{\text{ave}}$  is the arithmetic average of  $\Delta U_0^Z$  and  $\Delta U_0^{Z+1}$ . All energies are in eV.

	$U_1$	$2u$	$\Delta U_0^Z$	$\Delta U_0^{Z+1}$	$\Delta U_0^{\text{ave}}$	$\Delta E_{\text{Hund}}$	$U$
NiO	5.3	2.4	4.7	0.5	2.6	0.0	10.3
CoO	4.5	2.5	3.8	-0.6	1.6	1.9	10.5
FeO	4.1	2.3	2.8	-1.8	0.5	2.9	9.8

without the  $Z+1$  approximation and  $\Delta U_0^{Z+1}$  with the  $Z+1$  approximation in the final state—and they differ by  $\sim 4$  eV. It seems that the latter procedure is more appropriate here, since the energetics are such that the value of  $U_1$  in the final state affects the calculated spectra much more strongly than the  $U_1$  value in the initial state. But it is also true that  $Z+1$  approximation usually overestimates the effect of a core hole, so we will use the average of  $\Delta U_0^Z$  and  $\Delta U_0^{Z+1}$  in our estimate using Eq. (7).

In Tables III and IV, respectively, we list the values of  $\Delta_1$  and  $U_1$  obtained from the fit of the  $2p_{3/2}$  core-level spectra, and the values of the valence-band parameters  $\Delta$  and  $U$  estimated by using Eqs. (4) and (7), along with the necessary parameters such as  $u$ ,  $E_{\text{Hund}}$ , and  $\Delta U_0^{\text{ave}}$ . The values of  $\Delta$  and  $U$  for NiO are compared reasonably well with the published estimates based on the analysis of valence-band photoemission spectra<sup>8,24</sup> and BIS spectra.<sup>7</sup> The  $U$  value estimated here is a little larger than those estimates, but there are good reasons to believe that our estimate of  $U$  is the upper bound, whereas our  $\Delta$  value can be considered as a lower limit. The reasons are (i) we assumed the purely ionic configuration when estimating the value of  $\Delta U_0$ , but any screening by the conduction  $s$  electrons will reduce this value; (ii) the Hund's rule energy correction in both  $U$  and  $\Delta$  is most likely an overestimation because the lowest-energy multiplet will contribute to the determination of spectra most strongly. We can also see that the  $U$  values for CoO and FeO given in Table IV are consistent with the measured satellite positions of their valence-band spectra,<sup>18,28</sup> which are located at 10–12 eV below the valence-band maximum. This is especially true if we consider the  $U$  values as upper limits. We might note here that the energy separation between the  $d^{n-1}$  spectral weight in the valence-band XPS and the  $d^{n+1}$  spectral weight in BIS is larger than the  $U$  value by a few eV due to the hybridization shifts.<sup>29</sup>

In all these oxides, we see that the values of  $U$ 's and  $\Delta$ 's are larger than the  $3d$  band dispersional width,<sup>3,28</sup> which can explain the insulating property of these monoxides. Furthermore, the Coulomb correlation energies  $U$ 's are larger than the charge-transfer energies  $\Delta$ 's, so these oxides are in the charge-transfer regime according to the classification of Ref. 10. That is, these oxides are not the commonly believed conventional Mott-Hubbard insulators, but rather the band gap is mainly of the charge-transfer type, in agreement with the recent work of Ref. 14 and Ref. 18.

## B. Band gaps

According to the theoretical scheme of Zaanen, Sawatzky, and Allen,<sup>10</sup> the band gap of the transition-metal compounds in the charge-transfer regime within the cluster model is given by

$$E_G = \Delta + \delta - \frac{W}{2}, \quad (9)$$

where  $E_G$  is the band gap,  $W$  is the anion dispersional bandwidth, and  $\delta$  is the covalency effect arising from the  $d$ - $L$  hybridization.  $\delta$  can be expressed as  $\delta = 2\delta^n - \delta^{n-1} - \delta^{n+1}$  where  $\delta^n$ ,  $\delta^{n-1}$ , and  $\delta^{n+1}$  denote the energy lowering due to the  $d$ - $L$  hybridization of the lowest eigenstates of the initial state ( $N$ ), the ionized state ( $N-1$ ), and the electron affinity state ( $N+1$ ), respectively, (see Fig. 1). The values of  $\delta^n$ ,  $\delta^{n-1}$ , and  $\delta^{n+1}$  can be calculated from the corresponding effective model Hamiltonians whose diagonal matrix element energy positions are given in Fig. 1. But we have to use  $\Delta_1$  and  $U_1$  in place of  $\Delta$  and  $U$  in these calculations, because the hybridization  $T$  only acts between states of neighboring transition-metal and anion atoms.<sup>8</sup> We have done this calculation within the cluster approximation using the parameter values of  $\Delta_1$ ,  $U_1$ , and  $T$  given in Table II, and we also have included the Hund's rule energy contributions and  $\Delta U_0^{\text{ave}}$  of Table IV in the diagonal matrix element energies. The anion bandwidth is taken as 4 eV for oxides, and the value for  $\Delta$  is taken from Table III. The metal  $3d$  dispersional bandwidth  $w$  ( $w \leq 0.5$  eV for late transition-metal oxides) is neglected in the above expression of the band gap.

The estimated band gaps for the late transition-metal monoxides NiO, CoO, and FeO thus calculated are listed in Table V along with the experimental values. The experimental band gap for NiO was taken from Ref. 7, where the conductivity gap was determined from the comparison of photoemission and inverse photoemission spectra. The band gaps for CoO and FeO were taken from Refs. 30 and 31, respectively. These values, however, should be viewed with caution, because they were determined from optical spectroscopic measurements and may represent exciton binding energies instead of true band gaps. In fact, for the case of NiO, the band gap determined by optical spectroscopy in Ref. 30 was 3.8 eV, which is 0.5 eV less than that quoted in Ref. 7. We believe this difference reflects the excitonic effects resulting

TABLE V. The estimation of the band gap  $E_G$  from the value of  $\Delta$  in Table III and the anion bandwidth  $W$  of 4 eV (for oxides) or 3 eV (for dihalides).  $\delta$  denotes the  $d$ - $L$  hybridization shifts calculated using the parameter values of Table II as explained in the text. All energies are in eV.

	$\Delta$	$\delta$	$\frac{W}{2}$	$E_G$ (estimated)	$E_G$ (experimental)
NiO	6.2	-0.3	2.0	3.9	4.3
CoO	6.0	-0.8	2.0	3.2	3.0
FeO	4.9	-0.8	2.0	2.1	2.4
NiCl <sub>2</sub>	5.2	-0.1	1.5	3.6	4.7
NiBr <sub>2</sub>	3.7	0.3	1.5	2.5	3.5
NiI <sub>2</sub>	2.4	0.9	1.5	1.8	1.8

from the Coulomb attraction energy  $u$ . A similar effect should be present in CoO and FeO as well. With these uncertainties in mind, we can say that the estimated band gaps are in very good agreement with the experimental values and show the correct trend. We also have done a similar estimation of the band gaps of Ni dihalides using our  $2p$  XPS parameters, and compare them with the experimental data<sup>9</sup> in the same table. The experimental values were determined from the photoconductivity measurements, so they should represent the true band gaps. We again find that the estimated values are generally in reasonable agreement with the experimental values and show the correct trend depending on the ligand. It is quite reassuring to see that the calculated values are in fair agreement with the measured band gaps despite the simplicity of the calculation and the possible errors in the estimates of the parameter values. This probably means that the model used here catches the essential physics of the problem.

## V. CONCLUSIONS

We have analyzed the satellite structures of the transition-metal  $2p$  core-level photoemission spectra for the late transition-metal monoxides NiO, CoO, and FeO within the charge-transfer model and its cluster approxi-

mation. We found that the obtained model parameter values for monoxides show reasonable trends along the metal ions as well as along the ligands, including halogen and oxygen. With these parameters and some physical considerations, we have estimated the  $d$ - $d$  correlation energy and the charge-transfer energy related to the valence-band electronic structures, and concluded that these monoxides are not Mott-Hubbard insulators in their original sense but belong to the class of the charge-transfer-type insulators according to the scheme of Zaanen, Sawatzky, and Allen.<sup>10</sup> We have also gone further to estimate the band gaps of these oxides and Ni dihalides using our parameters. The estimated values are in fair agreement with the experimental values, and show the correct trend depending on the compounds. This gives us confidence that the model of Zaanen, Sawatzky, and Allen<sup>10</sup> applies to these monoxides, and that we can get information on the valence electronic structures of these highly correlated systems from the analysis of the core-level XPS satellite structures.

## ACKNOWLEDGMENTS

We thank Professor J. W. Allen and Professor G. A. Sawatzky for useful discussions. This work was supported in part by the grant from the Ministry of Education, Korea.

\*Author to whom all correspondences should be addressed.

<sup>1</sup>N. F. Mott, Proc. Phys. Soc. London Sect. A **62**, 416 (1949).

<sup>2</sup>J. Hubbard, Proc. R. Soc. London Ser. A **276**, 238 (1963); **277**, 237 (1964); **281**, 401 (1964).

<sup>3</sup>L. F. Mattheiss, Phys. Rev. B **5**, 290 (1972); **5**, 306 (1972).

<sup>4</sup>D. Adler and J. Feinleib, Phys. Rev. B **2**, 3112 (1970).

<sup>5</sup>G. K. Wertheim and S. Hüfner, Phys. Rev. Lett. **28**, 1028 (1972).

<sup>6</sup>K. S. Kim, Chem. Phys. Lett. **26**, 234 (1974).

<sup>7</sup>G. A. Sawatzky and J. W. Allen, Phys. Rev. Lett. **53**, 2339 (1984).

<sup>8</sup>A. Fujimori, F. Minami, and S. Sugano, Phys. Rev. B **29**, 5225 (1984); A. Fujimori and F. Minami, *ibid.* **30**, 957 (1984).

<sup>9</sup>C. R. Ronda, G. J. Arends, and C. Haas, Phys. Rev. B **35**, 4038 (1987).

<sup>10</sup>J. Zaanen, G. A. Sawatzky, and J. W. Allen, Phys. Rev. Lett.

**55**, 418 (1985); J. Magn. Magn. Mater. **54 - 57**, 607 (1986).

<sup>11</sup>S. Hüfner, J. Osterwalder, T. Riesterer, and F. Hulliger, Solid State Commun. **52**, 793 (1984).

<sup>12</sup>S. Hüfner, T. Riesterer, and F. Hulliger, Solid State Commun. **54**, 689 (1985).

<sup>13</sup>G. van der Laan, C. Westra, C. Haas, and G. A. Sawatzky, Phys. Rev. B **23**, 4369 (1981).

<sup>14</sup>J. Zaanen, C. Westra, and G. A. Sawatzky, Phys. Rev. B **33**, 8060 (1986).

<sup>15</sup>J. Park, S. Ryu, M. Han, and S.-J. Oh, Phys. Rev. B **37**, 10867 (1988).

<sup>16</sup>S. Sugano, Y. Tanabe, and H. Kimura, *Multiplets of Transition Metal Ions in Crystal* (Academic, New York, 1970).

<sup>17</sup>G. W. Pratt, Jr. and Roland Coelho, Phys. Rev. **116**, 281 (1959).

<sup>18</sup>A. Fujimori, N. Kimizuka, M. Taniguchi, and S. Suga, Phys.

- Rev. B **36**, 6691 (1987).
- <sup>19</sup>E. Sacher, Phys. Rev. B **34**, 5130 (1986).
- <sup>20</sup>S. Sugano and R. G. Schulman, Phys. Rev. **130**, 517 (1963).
- <sup>21</sup>G. A. Sawatzky, *Studies in Inorganic Chemistry*, edited by R. Meteselaar *et al.* (Elsevier, Amsterdam, 1982), Vol. 3.
- <sup>22</sup>J. Zaanen and G. A. Sawatzky, Phys. Rev. B **33**, 8074 (1986).
- <sup>23</sup>E. Antonides, E. C. Janse, and G. A. Sawatzky, Phys. Rev. B **30**, 1669 (1977).
- <sup>24</sup>J. Zaanen and G. A. Sawatzky, Can. J. Phys. **65**, 1262 (1987).
- <sup>25</sup>J. N. Plendl, L. C. Mansur, S. S. Mitra, and I. F. Chang, Solid State Commun. **7**, 109 (1969); J. Appl. Phys. **36**, 2446 (1965).
- <sup>26</sup>John C. Slater, *Quantum Theory of Atomic Structure* (McGraw-Hill, New York, 1960), Vol. 1, Chap. 16.
- <sup>27</sup>C. E. Moore, *Atomic Energy Levels*, Natl. Bur. Stand. (U.S.) Circular No. 467 (U.S. GPO, Washington, DC, 1958), Vols. 1-3.
- <sup>28</sup>Z.-X. Shen, J. W. Allen, P. A. P. Lindberg, D. S. Dessau, B. O. Wells, W. Ellis, J.-S. Kang, S.-J. Oh, A. Borg, I. Lindau, and W. E. Spicer, Phys. Rev. B **42**, 1817 (1990).
- <sup>29</sup>S. Hüfner, Solid State Commun. **53**, 707 (1985).
- <sup>30</sup>L. Messick, W. C. Walker, and R. Glosser, Phys. Rev. B **6**, 3941 (1972).
- <sup>31</sup>H. K. Bowen, D. Adler, and B. H. Auker, J. Solid State Chem. **12**, 355 (1975).